DESIGN AND ANALYSIS OF AN AUTONOMOUS ELECTRIC WING IN GROUND-EFFECT DRONE FOR SHIP CHANDLING

Ng Qi Heng[1], Chow Zhi Feng Reagan[2], Justin Teng Jia Ding[3], Chew Hong En[3], Wilson Lee Ying Jun[3]
[1]River Valley High School (Junior College), 6 Boon Lay Ave, Singapore 649961
[2]Anderson Serangoon Junior College, 4500 Ang Mo Kio Ave 6, Singapore 569843
[3]Defence Science Organisation National Laboratories, 12 Science Park Dr, Singapore 118225

Abstract
With limited docking space for resupplying, ship chandling offshore can provide Singapore a strategic advantage. With ground effect vehicles operating at faster speeds than boats, while experiencing less drag and more lift than conventional aircraft, they are perfectly suited for such short haul transportation. This project aims to explore the potential application of ground-effect vehicles for ship chandling through the design and analysis of a scaled down model. A traditional straight wing design was adopted with an anhedral angle and endplates to maximise the ground-effect's benefits. The prototype was modelled virtually using computed aided design (CAD) software to simulate its aerodynamic performance before a physical model was manufactured to test its structural soundness. Computational fluid dynamics simulations performed on the virtual model showed that it successfully achieved ground effect with a 30% increase in lift and reduction in drag when flying close to the ground. The physical model also demonstrated the design's structural soundness by sustaining minimal damage during multiple crashes during testing. Though more testing of the physical prototype is required to verify the accuracy of the simulations, overall the design has shown the potential to efficiently transport cargo over short distances.

1. Introduction
The ground effect occurs when aircraft fly at an altitude of less than half of their wingspan, experiencing increased lift and reduced induced drag (Halloran & O'Meara, 1999). A wing in ground-effect vehicle (WGEV) is an aircraft that capitalises on the ground effect by cruising near the ground. The increased payload capacity and fuel economy provided by the ground effect makes WGEVs more efficient at short haul transport than conventional aircraft. WGEVs also cruise at much higher speeds than most cargo ships,making them the ideal middle ground for high speed over-water transportation.

Ship chandling is the process where ships are supplied with the required necessities to operate (KaranC, 2021), like food and toiletries. With just 2 bases and a fleet of over 35 ships and submarines (RSN, 2022), resupplying the Republic of Singapore Navy's (RSN) entire fleet at these docks may prove challenging with such limited dock space. Ship chandling offshore, otherwise known as underway replenishment, can help alleviate this issue, with the additional benefit of reducing time and fuel wasted on turning into port and docking.

Currently underway replenishment is carried out with large frigates (RSN, 2022), which can take a relatively long time to reach the resupplying ship with a top speed of only around 25 knots (RSN, 2022). With WGEVs cruising at much higher velocities than such ships, a series of small resupply ground-effect drones could potentially increase the RSN's logistical efficiency and reduce its reliance on port availability.

2. Literature Review

This literature review aims to explore existing literature surrounding WGEVs for a comprehensive contextualisation, unveiling possible directions for advancement of this technology.

2.1 Key Attributes of the WGEVs

The reduced induced drag experienced by WGEVs is a result of disruption to wingtip vortex formation. Normally, an aircraft's wingtip vortices produce a downwash of air onto the wing, effectively increasing the angle of the relative airflow and increasing the downstream component of lift, otherwise known as induced drag. In ground effect, wingtip vortex formation is inhibited due to obstruction by the ground (SkyBrary, 2019), reducing the effective angle of attack and minimising induced drag. Thus, in theory, a lower induced drag would allow the aircraft to travel more efficiently.

Another key feature of the WGEVs is its increased lift. A plane generates a lift force by pushing an incoming air mass downwards. Following Newton's 3rd Law, the "turned" airflow creates a resultant force upwards on the wing. The increased lift observed in WGEVs as compared to conventional aircraft can be attributed to "ram pressure". The wing of the WGEV slows down incoming air by exerting a "ramming force", deflecting and compressing the air below the wing. With the ground or water surface obstructing the downward flow of air, spiralling eddies form below the wing, increasing air pressure and lift.

2.2 Stability and control of WGEVs

The earlier discussion on key features of the WGEVs may lead to raised concerns regarding the longitudinal stability of the aircraft, especially when the increased lift is taken into consideration. To further elaborate on this point, the increased lift results in a higher pitching moment (Halloran & O'Meara, 1999), defined as the moment created about the aerodynamic centre of the wing caused by the movement of a wing through the air. This pitching moment, which is due to the pressure distribution on the surface of the wing, needs to be balanced for longitudinal equilibrium to be achieved on the aircraft. With increased lift, the pitching moment from the wings is exacerbated in the ground effect , requiring larger stabilisers that increase weight and drag. A solution employed by some WGEVs, like the Russian ekranoplan, is a high tail outside the ground effect, allowing it to produce a stronger counter-moment to stabilise the WGEV longitudinally (Dole & Lewis, 2000).

Additionally, directional control is another pertinent issue facing WGEVs. The proximity to the ground limits the WGEV's maximum bank angle, reducing its capacity for rolling and increasing its reliance on yawing for directional control, possibly increasing its turning radius and inhibiting its manoeuvrability. However, with large vertical control surfaces, the necessity of banking for sharp turns may be reduced.

2.3 Existing WGEVs

Among the more pre-eminent attempts by the militaries of the 20th century to create an effective model of the WGEV was the Lun-class ekranoplan (Yun et al., 2009), designed in 1975 and later used in the Soviet military in the 1980s and 1990s, which utilised large endplates to force and trap more air underneath the wings to increase the "ram pressure". While the ekranoplan

managed a record-breaking maximum speed of 550 kmh^{-1}, there were multiple flaws that ultimately prevented its widespread usage. The ekranoplan, being an early pioneer for WGEVs, was unable to transport goods and supplies under turbulent conditions. It was this fact that made its use in the open sea completely out of the question, negating much practical application. In addition, the craft's inability to orient itself through rolling significantly hindered its ability to make sharp turns, making obstacle avoidance another problematic issue.

A more recent attempt to revitalise the concept of WGEVs came in the form of the Airfish 8 (Matdaud et al., 2019) created by a Singapore-based company known as Wigetworks. It is expected to be able to carry up to 10 people due to the immense lifting capacity of the ground effect. Unlike its massive predecessor, the Airfish 8 is considerably smaller, featuring a reverse delta wing design that is longitudinally stable, allowing for more comfortable rides. However, being a relatively new design and theoretically a vast improvement from the ekranoplan, the Airfish 8 has (as of 2022) yet to undergo extensive testing required to determine important attributes, including but not limited to cargo capacity, fuel consumption and overall efficiency.

With few well-known designs in use currently, WGEV technology is still in its infancy and has yet to reach its full potential (Taylor et al., 2004). Thus this project hopes to further study and optimise this platform through exploring one of its potential applications.

3. Materials and methods

3.1 Objectives and performance targets

The objective of this project is to design a scaled down proof of concept prototype WGEV to assess the feasibility of their application for ship chandling.

The designed WGEV aims to carry high payloads over short distances to ships offshore, thus a high payload capacity is required. The maximum takeoff mass (M_{TO}) of the model was thus sized to be 1.5kg, in order to accommodate all electronics and a small payload of 500g.

To maximise the effect of the ground effect, the aircraft will fly as close to the ground as possible with a ground clearance (h/c) of 0.2 (Kwang et al., 2008), which is defined as the distance from the lowest point of the aircraft to the ground divided by the chord length. This helps to prevent the WGEV from colliding with small objects on the ground.

To navigate crowded waters, it should be able to glide as slowly as possible to reduce its turning radius and prevent crashes. Thus, a cruise speed slightly slower than the typical remote control aircraft was selected for greater manoeuvrability.

Performance attribute	**Symbol**	**Value**
Maximum takeoff mass	M_{MTO}	1.5 kg
Cruise height	h_{CR}	2 cm
Cruise speed	V_{CR}	8 ms^{-1}

Figure 3.1: Table of performance targets for the aircraft

3.2 WGEV Configuration

A traditional straight wing aircraft configuration was selected due to its relative ease of manufacturing compared to other unconventional configurations like the reverse delta wing, which required large wing ribs that are difficult and costly to produce.

Though the actual aircraft will be configured for over-water operations, the prototype was configured with landing gear in a taildragger formation for ground operations to test its aerodynamic and structural capabilities.

Three foils were considered for the wing; the popular NACA 4412, NACA 6409 and the NACA 6409 with a 10 degree flap (Figure 2.2). The NACA 4412's popularity stems from its relatively flat bottom that is easy to manufacture, and its relatively low drag coefficient. On the other hand, NACA 6409 and its flapped variant produce significantly more lift in ground effect due to their higher camber. The foil selection process is discussed further below, aided by results from computational fluid dynamics (CFD) simulations for each foil.

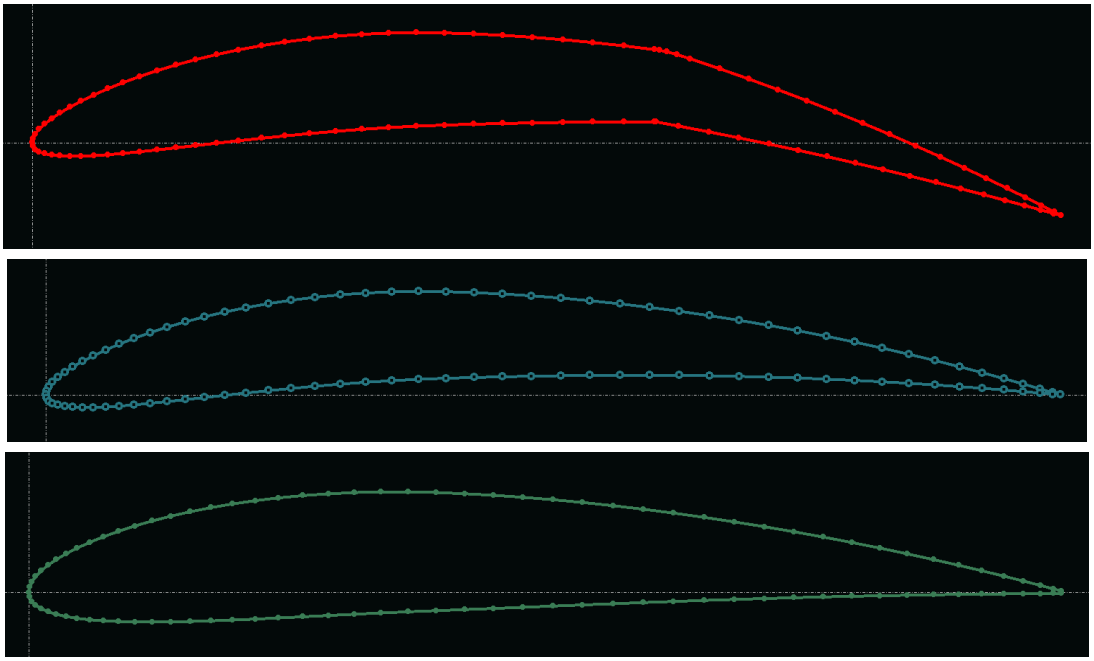

Figure 3.2: Diagrams of the Flapped NACA 6409, NACA 6409 and NACA 4412 airfoils

3.3 Structural Features

Our prototypes utilise a mix of polystyrene foam, aluminium, carbon fibre and 3D printed plastic, specifically polylactic acid (PLA) and acrylonitrile butadiene styrene (ABS) plastic.

For the outer surface of the prototype, polystyrene foam was chosen in favour of 3D printed PLA plastic and balsa wood due to its low density and flexibility to form complex shapes. The density of polystyrene foam was measured to be 0.170 g/cm^3, similar to balsa wood's 0.170 g/cm^3 but an order of magnitude lighter than relative to PLA's 1.25 g/cm^3. However, with a higher porosity of

about 98% (Arslan, 2017) relative to balsa wood's 89.5% (Jang & Kang, 2022), the internal structure of foam is less rigid and more flexible than balsa wood, allowing it to flexibly form more complex shapes that balsa wood cannot.

The wings of the prototype are created by wrapping foam around a wing skeleton, which are created using carbon fibre wing spars and 3D printed PLA wing ribs. Carbon fibre was the ideal due to its high tensile strength of 3 to 7 GPa and much lower density of under 2.2 g/cm^3 (Latifi, 2021) compared to aluminium's roughly 90MPa tensile strength and over 2.6 g/cm^3 density (aalco, 2019).

Other structural features like mounts and landing gear are manufactured and reinforced with plywood, PLA plastic, and aluminium metal as they have relatively high shear and compressive strengths, allowing them to be bolted down tightly to hold key components together.

3.3 Aerodynamic features

An anhedral angle is employed to create a high-pressure "air tunnel" underneath the wing, maximising lift (Lee et al., 2018). This anhedral is constrained by the ground clearance of the propeller during cruise and the wing's trailing edge when on the ground. To prevent the propeller from striking the ground, the aircraft must cruise with its fuselage at least 10 cm from the ground, thus limiting the ability of wings with smaller anhedrals. On the flip side, to prevent the wing's trailing edge from contacting the ground, the wing's pitch angle is restricted, inhibiting the amount of lift produced. The XFLR5 software was used to optimise this anhedral angle, with the results of this optimization being discussed below.

This "air tunnel" effect is enhanced by the implementation of endplates at the end of each wing, which help trap more air under the wings to increase the "ram pressure" and hence the lift generated (Lee et al., 2010).

3.4 Weight and balance

As the line of action of the wing's lifting force does not pass through the aircraft's centre of gravity (CG), the lift generates an upwards pitching moment. Thus, an appropriately sized horizontal stabiliser is deployed to generate a counter-moment to maintain the aircraft's longitudinal stability.

Similarly, the line of action of the aircraft's thrust also does not pass through the CG, generating a counter-clockwise moment in flight that has to be accounted for. This can be modelled with the Coefficient of moment (C_M), a dimensionless parameter used to quantify the moment generated by a force about the CG (Scholz, 2022).

let M_E be the moment generated by engine

C_{ME} be the coefficient of moment about engine

Moment arm of thrust = 0.031 m

Thrust in cruise = drag force = 2.0 N

$$M_E = 0.031 \times 2.0 = 0.062$$

$$C_{ME} = \frac{M_E}{qSc} = \frac{-0.062}{\left(\frac{1}{2}\times 1.225\times 8^2\right)(0.240)(0.200)} = \quad -0.03$$

Thus the aircraft's main wing and horizontal stabiliser must have a combined C_M of 0.03 inflight to maintain longitudinal stability.

Additionally, the CG is positioned slightly offset from the neutral point of the aircraft, giving the CM curve a negative gradient (Figure 3.3) and causing the aircraft to naturally correct its angle of attack (AoA) to 0°, thus providing it with natural longitudinal stability.

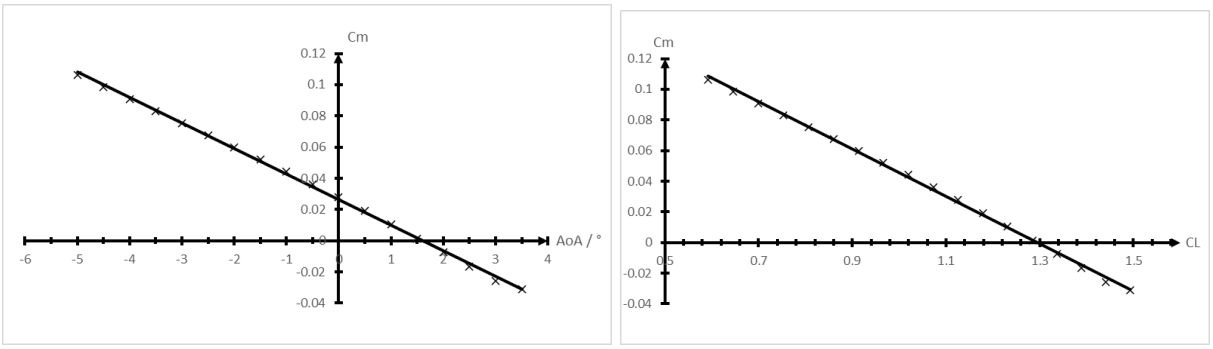

Figure 3.3: Impact of AoA (Left) and Cl (Right) on the WGEV's natural Cm

4. Results

XFLR5 was initially used to size the main wing and empennage. Fusion 360 was then used to virtually model the aircraft's shape and centre of gravity before a physical prototype was made. Finally, fusion CFD was utilised to analyse the airflow and pressure around the aircraft with a virtual wind tunnel.

4.1 Aircraft sizing and optimisation

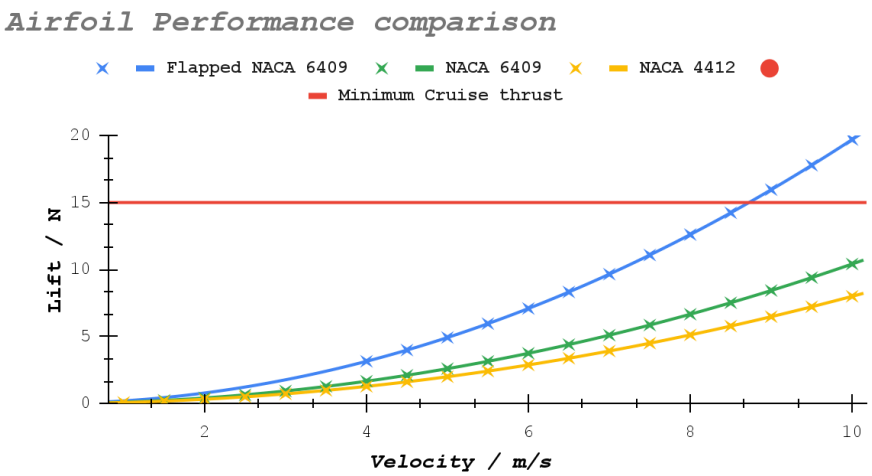

Figure 4.1: Comparison of lift generated by each foil at varying velocities

To compare the airfoils, a wing with a 1.2m span and 0.2m chord was modelled in XFLR5 for each foil. With the flapped NACA 6409 producing significantly more lift at the target velocity than the other 2 foils, it was selected as the foil for the prototype.

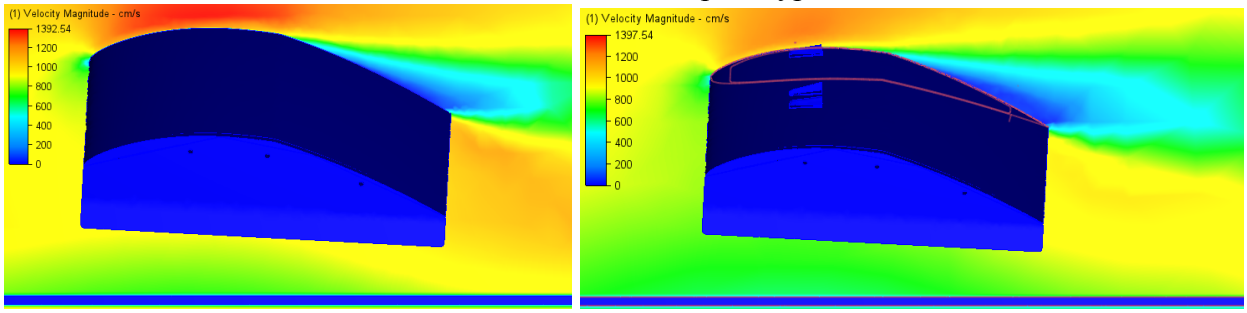

Figure 4.2: Flow separation without (left) and with (right) vortex generators

Due to the flapped NACA 6409 relatively high camber, flow separation occurs at the wing's trailing edge (Figure 4.2) as the air's momentum prevents it from following the cambered surface downwards. Vortex generators were considered to mix the high energy free stream above with the low energy boundary layer (Udris, 2015). However they had minimal impact on the flow separation (Figure 4.2) and thus were not implemented in the actual prototype to reduce drag.

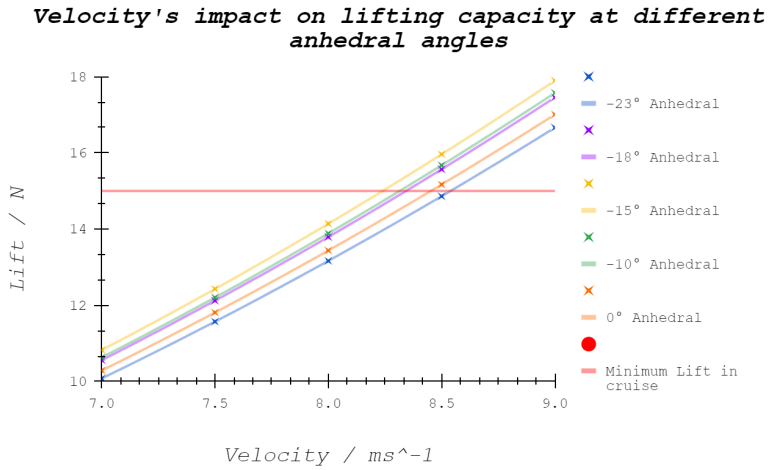

Figure 4.3: Graph highlighting effect of anhedral on lifting capacity

Due to the 2 constraints mentioned above, the lifting capacity of the wing increases as the anhedral angle approaches 15 degrees, where the lift produced hits a peak (Figure 4.3). Thus a 15 degree anhedral was applied to the prototype's wing.

4.2 Physical model

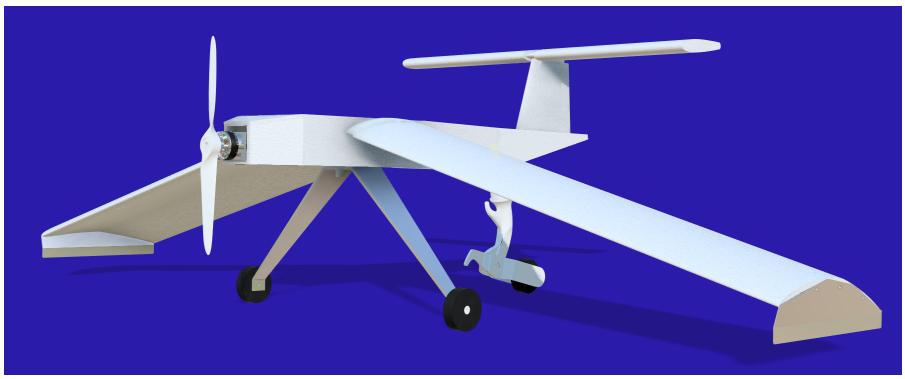

Figure 4.4: 3D model of prototype

Figure 4.5: Image of physical prototype

Test	Events	Damage Sustained
1	Prototype travelled forward in a straight line at low throttle. It then veered sharply leftwards upon setting full throttle.	NIL
2	Prototype gradually veered left as throttle increased. Main landing gear buckled and caused aircraft to "hop" up momentarily before landing safely.	Main landing gear was bent and the gear spar fell off
5	Prototype travelled in a straight line before veering sharply to the right from pilot inputs. Prototype rolled counter-clockwise while veering, causing the left main gear to buckle and bend, causing prototype to flip as wheel touched the gear mount and suddenly experienced more friction,	Main landing gear slightly bent
8	Prototype moved slightly before flipping over about the main landing gear	Horizontal stabiliser slightly tilted

Figure 4.6: Record of notable flight tests

The aircraft was split into several components which were manufactured separately; The fuselage, left and right wings, empennage, rear gear and main gear (Figure 4.4). Once modelled, the designs were translated into a physical model (figure 4.5), which was driven around to test the model's structural soundness. Video footage of each test was recorded to compile records on the damage received by the prototype and their causes (figure 4.6).

4.3 CFD analysis

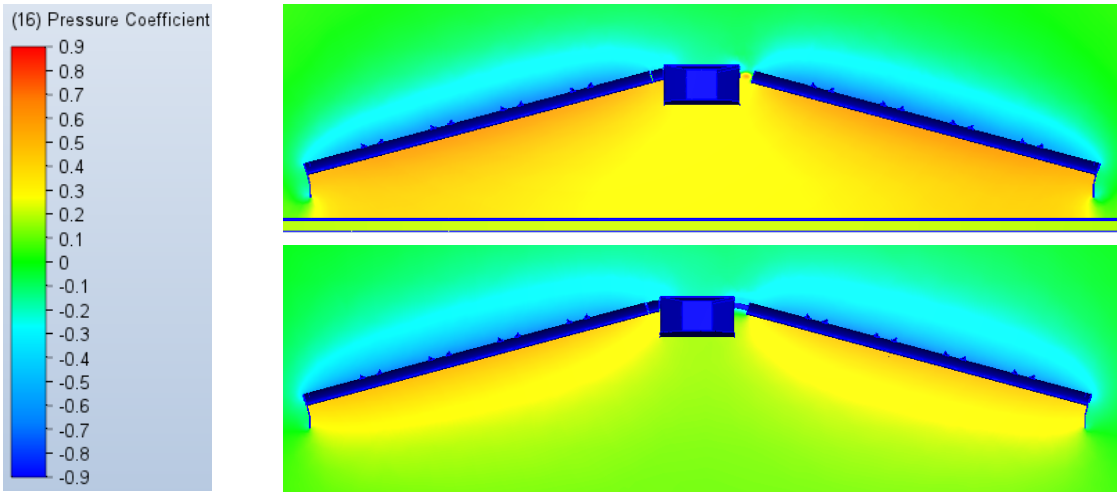

Figure 4.7: High pressure zone underneath wing inside (above) and outside (below) ground effect

For this analysis, the inlet airflow velocity is set to 10 ms^{-1} while the outlet air pressure is set to 0 Pa (gage). The pressure coefficient of the air underneath the wing in ground effect is higher than that of the wing not in ground effect (Figure 4.7), thus showing that our prototype is able to achieve ground effect. This is corroborated by simulations from XLFR that show the model in ground effect experiencing 30% more lift and 30% less drag.

5. Discussion

5.1 Achieving ground Effect

The primary objective of applying ground effect was accomplished through simulations run on Fusion CFD. As seen in the above CFD analysis, the larger pressure coefficient under the wings demonstrated that in theory, ground effect can be achieved using this design.

However, empirical data to support the simulations currently cannot be obtained as the prototype is unable to reach the minimum velocity takeoff velocity of 8m/s without veering off. Hence, improvements to the yaw stability must be made by increasing the vertical stabiliser's size and moment arm. With this improvement, further testing for ground effect can be conducted.

5.2 Structural integrity

The physical prototype was able to survive multiple drops and flips during testing with minimal damage to most components apart from the main landing gear (figure 4.6), thus proving that the model is structurally sound.

As mentioned, the main gear was relatively weak and began to flex after a few crashes due to aluminium's flexibility and relatively low young's modulus. Thus better materials like PLA can be considered for the main gear for increased rigidity, though other factors like compressive strength must be considered to ensure the gear stays intact after a hard landing.

Additionally, the wings also tended to flex slightly when loaded despite the rigid double carbon fibre spar. This is possibly due to the spars cutting into the PLA plastic of the wing mount and giving itself space to flex. A possible resolution to this is the implementation of a wing box that allows for a longer length of spar to be inserted into and supported by itself, thus preventing the load on the wing from cutting the joint and allowing the wing to flex.

6. Limitations and future work

Due to the size constraints of the 3D printers available, the wing ribs' chord length was limited to 200mm, preventing the implementation of other aircraft configurations like the reverse delta wing which requires much longer root chord lengths for an aircraft this size. Thus future work can explore other production methods like the usage of a computer numerical control (CNC) cutter to cut out larger wooden ribs.

Additionally time constraints prevented the implementation of several autonomous features, which are explored more in our partner project's. Thus future studies can explore the possibility

of proportional integral derivative (PID) control and pathfinding algorithms to increase the platform's autonomy.

7. Acknowledgements

We wish to express our utmost gratitude to our mentors Justin, Hong En and Wilson for their guidance and advice regarding the aircraft's design and manufacturing; the Defence Science Organisation (DSO) and the Young Defence Scientists Program (YDSP) for providing us the resources and opportunity to carry out this project; our partner team consisting of Vera and Enrui who helped tirelessly with the manufacturing and testing of the aircraft; the many DSO staff and interns who provided tips, advice and offered a helping hand throughout this project, including Eugenia, Calvin, Desmond, Nick and many more.

References

aalco. (2019). *Aluminium Alloy Specifications*. Aluminium Alloy Specifications. https://www.aalco.co.uk/datasheets/Aalco-Metals-Ltd_Aluminium-Alloy-Specifications_42.pdf.ashx

Arslan, D. (2017). *How much porosity is in polystyrene foam?* ResearchGate. Retrieved December 29, 2022, from https://www.researchgate.net/post/How_much_porosity_is_in_polystyrene_foam

Dole, C. E., & Lewis, J. E. (2000). *Flight Theory and Aerodynamics: A Practical Guide for Operational Safety*. Wiley.

Halloran, M., & O'Meara, S. (1999). *Wing in Ground Effect Craft Review*. Wing in Ground Effect Craft Review. https://apps.dtic.mil/sti/pdfs/ADA361836.pdf

Jang, E.-S., & Kang, C.-W. (20 22). Porosity analysis of three types of balsa (Ochroma pyramidale) wood depending on density. *Official Journal of the Japan Wood Research Society*, *68*(31). https://jwoodscience.springeropen.com/articles/10.1186/s10086-022-02037-2#:~:text=Pan%20et%20al.,with%20porosity%20of%20approximately%2089.5%25.

KaranC. (2021, July 25). *Who is a Ship Chandler?* Marine Insight. Retrieved December 29, 2022, from https://www.marineinsight.com/careers-2/who-is-a-ship-chandler/

Kwang, H. J., Ho, H. C., & Hee, J. K. (2008). Experimental investigation of wing-in-ground effect with a NACA6409 section. *J Mar Sci Technol*, *2008*(13), 317-327. https://d1wqtxts1xzle7.cloudfront.net/50424225/s00773-008-0015-420161119-30663-rjawxa-libre.pdf?1479596228=&response-content-disposition=inline%3B+filename%3DExperimental_investigation_of_wing_in_gr.pdf&Expires=1672310034&Signature=c6wDNdMeMfaTTZTAnowXCcok

Latifi, M. (Ed.). (2021). *Engineered Polymeric Fibrous Materials*. Elsevier Science.

Lee, J., Han, C., & Bae, C.-H. (2010). Influence of Wing Configurations on Aerodynamic Characteristics of Wings in Ground Effect. *JOURNAL OF AIRCRAFT*, *47*(3), 1030-1040. https://citeseerx.ist.psu.edu/viewdoc/download?doi=10.1.1.167.7330&rep=rep1&type=pdf

Lee, T., Tremblay-Dionne, V., & Ko, L. (2018). Ground effect on a slender reverse delta wing with anhedral. *Journal of Aerospace Engineering*, *0*(0), 1-10. 10.1177/0954410017754147

Matdaud, Z., Zhahir, A., Pua'at., A. A., Hassan, A., & Ahmad, M. T. (2019). Stabilizing Attitude Control For Mobility Of Wing In Ground (WIG) Craft - A Review. *IOP Conf. Series: Materials Science and Engineering*, *642*. https://iopscience.iop.org/article/10.1088/1757-899X/642/1/012005/pdf

RSN. (2022, April 29). *Home*. YouTube. Retrieved January 1, 2023, from https://www.mindef.gov.sg/web/portal/navy/navy-life/life-at-sea/ep6/!ut/p/z1/lZDBDoIwEES_hS_o7rYiPbYREZRgaSrYi-FEmih6MH6_xnCQC-reJnkzsxnmWcv80D1C393DdejOL3308QnNVqBIaJcoh2CWYqGsjVFbZM0bgMkp0DVpDpBVxPz__s-k3_wzgJ-Pb5ifVoA0KRiuDvuyKpBSPgLSyAwwobJa1ytQBcpc8A1

RSN. (2022, 12 15). *Home Page*. MINDEF Singapore. Retrieved January 1, 2023, from https://www.mindef.gov.sg/web/portal/navy/

Scholz, D. (2022, November 5). *Aircraft Design for HOOU@HAW*. HAW Hamburg. Retrieved

December 29, 2022, from https://www.fzt.haw-hamburg.de/pers/Scholz/HOOU/

SkyBrary. (2019). *Ground Effect*. SKYbrary. Retrieved July 17, 2022, from https://skybrary.aero/articles/ground-effect

Taylor, G., Matjasic, K., & Flugmechanik, F. (2004). TURNING SEAWAYS INTO FREEWAYS THE 90 KNOT ZERO-WASH FERRY TURNING SEAWAYS INTO FREEWAYS THE 90 KNOT ZERO-WASH FERRY. *Pacific 2004 International Maritime Conference*. https://www.researchgate.net/publication/341152623_TURNING_SEAWAYS_INTO_FREEWAYS_THE_90_KNOT_ZERO-WASH_FERRY_TURNING_SEAWAYS_INTO_FREEWAYS_THE_90_KNOT_ZERO-WASH_FERRY

Udris, A. (2015, September 1). *Vortex Generators: Preventing Stalls At High And Low Speeds*. Boldmethod. Retrieved December 29, 2022, from https://www.boldmethod.com/learn-to-fly/aerodynamics/vortex-generators/

Yun, L., Bliault, A., & Doo, J. (2009). *WIG Craft and Ekranoplan: Ground Effect Craft Technology*. Springer US.